Research Article

Jiangmei Zhang, Xiang Gao*, Kunpeng Wang, Youyong Liu, Xiuhong Yang, and Yihui Ao

Detection of the damage threshold of fused silica components and morphologies of repaired damage sites based on the beam deflection method

https://doi.org/10.1515/phys-2018-0070
Received Jan 29, 2018; accepted Jul 05, 2018

Abstract: This article proposes a method to quickly detect the damage threshold of the fused silica components and the characteristics of the repair point damage. With a device detecting the beam deflection, the laser damage threshold is detected, quickly and effectively. Then, based on the beam deflection though mitigated sites, the beam deflection signals of the damage repair points are measured and the morphologies of mitigated sites are analyzed. This method is helpful in the online assessment of the damage resistance of the downstream optics and provides the guidance of the repair process.

Keywords: Laser-induced breakdown; Beam deflection method; Optical materials

PACS: 42.62.-b, 42.70.Ce, 79.20.Ds

1 Introduction

The damage of the fused silica surface caused by ultraviolet laser has been the major cause that limits the development of the large aperture high-power laser system [1–3]. Accurately and effectively detecting the damage threshold is of great significance in assessing damage resistance of optical components. Traditional ways of measuring damage threshold include phase contrast microscope observation [4–6], plasma flashing [7], monitoring of the transmission [8, 9], photoacoustic technique [10] and light Scattering [11, 12], etc. The beam deflection method [13–16], which is usually applied in measuring the damage threshold of thin film coating, is not often applied in detecting the damage threshold of fused silica. It is the most effective way to repair the damaged fused silica optimal components by applying CO_2 laser irradiation thus restricting the growth of the damaged fused silica optimal components. However, CO_2 laser treatment [17, 18] is to remove the damaged materials in this way of fusing or evaporating, thus forming a Gaussian smooth pitch [19], which generates strong optical field modulation and possibly will cause the downstream components [9, 20]. The results show that optical field modulation growth is closely connected with the morphologies of mitigated sites, and it is imperative to detect the morphological properties of mitigated sites quickly and effectively in order to analyze the influence of the mitigated sites on the damage resistance of the downstream optics. This article proposes a quick and effective method of detecting the damage threshold of the fused silica components and the morphological properties of mitigated sites.

2 Experimental set of beam deflection

The experimental set of beam deflection can be seen in Figure 1. The samples are exposed to Nd:YAG pulse laser with 355 nm wavelength and pulse width of 10 ns (1/e). An energy detector (PE25) is used to detect laser energy. The combination of a half-wave plate and polarizer is used to control the energy of each harmonic beam. During the measurements, laser spots are casted to the front of the samples. He-Ne probe beam is casted from a certain angle to the laser region and the transmission light is, via a re-

***Corresponding Author: Xiang Gao:** Joint Laboratory for Extreme Conditions Matter Properties, Southwest University of Science and Technology and Research Center of Laser Fusion, CAEP, Mianyang 621010, China; Email: gaoxiang6969@163.com
Jiangmei Zhang, Kunpeng Wang, Youyong Liu, Xiuhong Yang: School of Information Engineering, Southwest University of Science and Technology, Mianyang 621010, China
Yihui Ao: Joint Laboratory for Extreme Conditions Matter Properties, Southwest University of Science and Technology and Research Center of Laser Fusion, CAEP, Mianyang 621010, China

flector, reflected into the quadrant detector to measure the laser spot displacement. In Figure 2, the probe beam are casted from three different angles. In mode A, the incident beam is casted to the edge of the laser spot and the emergent beam is far away from the edge of laser spots. In mode B, the incident beam and the emergent beam are all in the laser region. In mode C, the incident beam is far away from the laser spots, while the emergent beam is at the edge of laser spots.

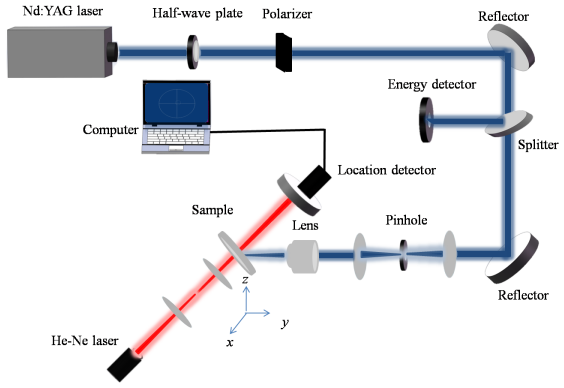

Figure 1: Experimental set of beam deflection

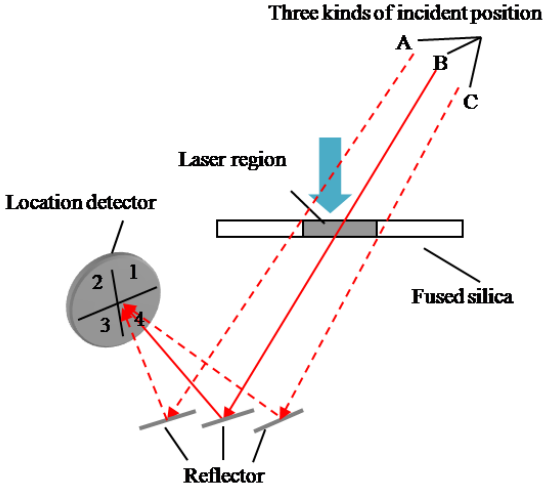

Figure 2: Three incidence modes of the probe beam

With the increase of irradiation time, the deflections of probe spot in the different modes are shown in Figure 3. In Figure 3(a), the three rows of the picture, from top to bottom, respectively denote the measuring results of mode A, mode B, and mode C. The four columns, from left to right, denote respectively the positions of the deflection beam, before working, 3 seconds later, 6 seconds later, and 9 seconds later. When the probe beam is casted in mode A, the deflection beam moves toward quadrant 1 and quadrant 4. When in mode B, the displacements of the deflection beam can't be clearly noticed. When in mode C, the deflection beam moves toward quadrant 2 and quadrant 3. In mode A and mode C, with the increase of irradiation time, the displacements enlarge accordingly, and become stable after a period of time. The three displacements of the deflection beam with the increase of irradiation time are shown in Figure 3(b). From Figure 3(b), when probe beams are casted in mode B, the displacements of deflection beam cannot be clearly noticed. When in mode C, the deflection beam moves toward quadrant 2 and quadrant 3. In mode A and mode C, with the increase of irradiation time, the displacements increase accordingly, and become stable after 12 seconds. To improve detection sensibility of the beam deflection, mode A and mode C are adopted to detect the displacements after the irradiation time of 12 seconds.

When laser damage occurs, the deflection displacement of probe beam will increase dramatically, 1-2 order of magnitudes. To verify the accuracy of detecting laser damage threshold with this method, the traditional phase contrast microscope observation is applied to compare the average fluence, respectively, at damage probability of 0%, 50% and 100%, which is shown in Table 1.

From Table 1, the discrepancy between the two methods is within 3%. The beam deflection method developed in this article can be applied to large-aperture, high-power laser systems to quickly detect laser damage threshold in situ. The shift of laser spot and the fluctuation of energy will cause uncertainty of the measurement. The energy detector connected to a computer is used to monitor the average energy of 100 pulses (during 10 seconds). The fluctuation of the measured fluence for each pulse is less than 2.5%. The changes in the microstructure and the refractive index of surrounding medium could occur on the surface of fused silica samples irradiated by the laser pulse with fluence near LIDT, which seriously shortens the lifetime of optical components. The size of these damage sites is too small to be observed by the phase contrast microscopy, used in the experiment, with a resolution of 1.5 μm for these minor sites. Thus, compared to analysis of morphologies, there is less uncertainty using beam deflection method, because this method can detect smaller damage site by adjusting the quadrant detector farther from the sample.

Table 1: Damage probability comparison

Damage probability		0%	50%	100%
Average fluence (J/cm^2)	Phase contrast microscope	9.5	19.3	25.4
	Beam deflection method	9.6	19.8	26.1

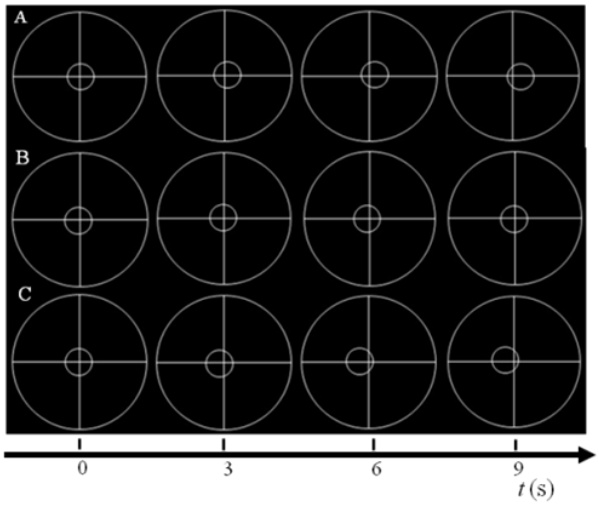

(a)

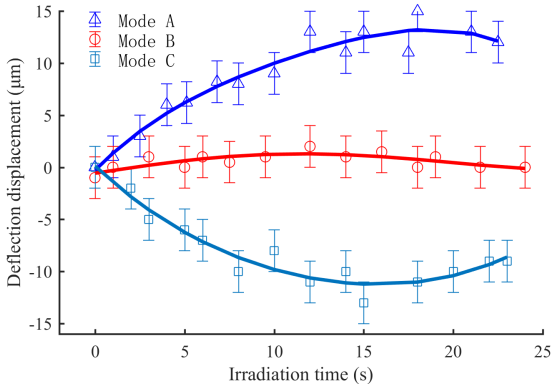

(b)

Figure 3: Deflection displacement of probe beams in the three modes with the growing irradiation time

3 Analysis of morphologies of mitigated sites

In the experiment, fused silica samples were 50 × 50 × 5 mm^{3}in size, with the surface roughness (RMS) of less than10 nm. The samples were immersed in HF solution first to remove the redeposition on the surface. Then, irradiated by the 355 nm wavelength and 300 μm diameter laser pulse, a mass of damage sites occur. The range of laser fluence used in the experiment is 5-27 J/cm^2 with the fluctuation of fluence ±3%. The damaged fused silica samples were immersed in ultra-high-purity HF solution repeatedly to remove the fragments, and irradiated by 97 W CO_2 laser with 7 mmin diameter and the irradiation time for 4 seconds. Subsequently, damage sites became smooth again. The mitigated sites has a Gaussian spatial profile, and their lateral sizes range from 50 μm to 550μm. Lastly, the deflection of the probe beam (He-Ne laser) passing the mitigated sites is detected by the location detector, which is shown in Figure 4.

The characteristics of mitigated sites $H(r)$ is denoted as [9]

$$H(r) = H_0 \exp\left(-\frac{r^2}{R_0^2}\right) \tag{1}$$

where, H_0 is the maximum repair depth, and R_0 is the effective half width (at 1/e).

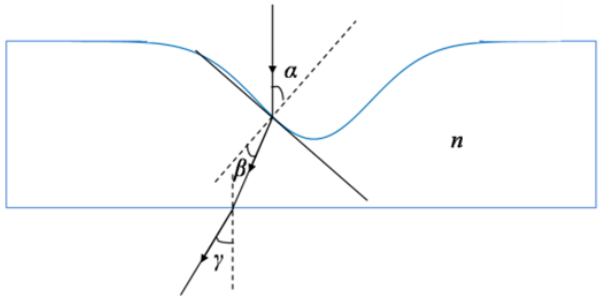

Figure 4: Deflection of the probe beam passing the mitigated sites

When the probe beam is vertically incident to a mitigated site as shown in Figure 4, the tangent value of incidence angle α is denoted as

$$\tan(\alpha) = \frac{dH(r)}{dr} = H_0 \frac{2r}{R_0^2} \exp\left(-\frac{r^2}{R_0^2}\right) \tag{2}$$

where

$$\begin{cases} \sin(\alpha) = \tan(\alpha)/\sqrt{1+\tan^2(\alpha)} \\ \cos(\alpha) = 1/\sqrt{1+\tan^2(\alpha)} \end{cases} \tag{3}$$

From the refraction theorem:

$$\sin(\beta) = \sin(\alpha)/n = \tan(\alpha)/n\sqrt{1+\tan^2(\alpha)}, \tag{4}$$

$$\cos(\beta) = \sqrt{1 - \tan^2(\alpha)/n^2[1 + \tan^2(\alpha)]}, \tag{5}$$

Where β is the refraction angle and n is the refractive index of the medium. According to angle conversion, the sine value of the emergent angle γ can be denoted as

$$\begin{aligned} \sin(\gamma) &= n\sin(\alpha - \beta) \\ &= n\left[\sin(\alpha)\cos(\beta) - \sin(\beta)\cos(\alpha)\right]. \end{aligned} \tag{6}$$

The distance from the samples to the position detector is d, and the deflection displacement can be denoted as

$$S = d\tan(\gamma) = d\sin(\gamma)/\sqrt{1 - \sin^2(\gamma)}. \tag{7}$$

When $d[\tan(\alpha)]/dr = 0$, which means that $r = (1/2)^{1/2}R_0$, the deflection displacement takes its maximum value. Then, equation (2) can be rewritten as

$$\tan(\alpha) = H_0\frac{\sqrt{2}}{R_0}\exp\left(-\frac{1}{2}\right). \tag{8}$$

The data measured by the stylus profilometer indicates that the depth of mitigated sites is much smaller than their width (H_0 << R_0, that is, $\tan(\alpha)$ <<), and the results of equations (3), (4) and (5) can be simplified as

$$\begin{cases} \sin(\alpha) \approx H_0\frac{\sqrt{2}}{R_0}\exp\left(-\frac{1}{2}\right) \\ \sin(\beta) \approx H_0\frac{\sqrt{2}}{nR_0}\exp\left(-\frac{1}{2}\right) \\ \cos(\alpha) \approx 1 \\ \cos(\beta) \approx 1 \end{cases} \tag{9}$$

Applying equations (6) and (9), the maximum deflection displacement according to equation (7) can be expressed as

$$S_m \approx d(n-1)H_0\frac{\sqrt{2}}{R_0}\exp\left(-\frac{1}{2}\right). \tag{10}$$

From equation (10), the maximum value of deflection displacements grows with the growing repair points pitch depth. However, the maximum value of deflection displacements decreases with the enlarging repair points width.

Figure 5 indicates the deflection displacements of two different types of mitigated sites at different points. With the probe beam moving toward repairing pitches, the deflection displacements increase first and then decrease. With the beam moving to the bottoms of repairing pitches, the deflection displacements reversely increase first and then decrease. With the beam shifting out of mitigated site, deflection signals return to the equilibrium position.

Figure 6 reveals the changes of maximum deflection with depth-to-width ratios. The experiment values have good agreement with the results from equation (10), which

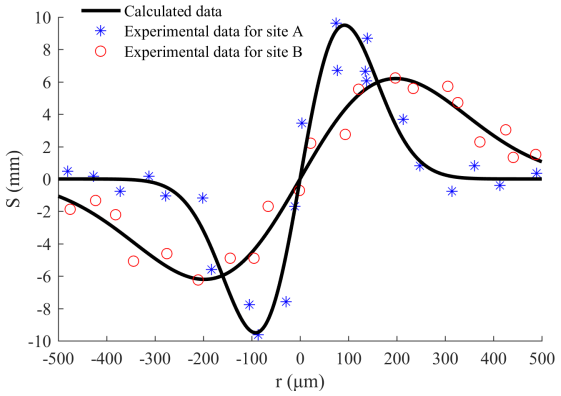

Figure 5: Deflection displacements of two different types of mitigated sites at different positions (Site A R_0 = 130 μm, H_0 = 3.2 μm; Site B R_0 = 280 μm, H_0 = 4.5 μm)

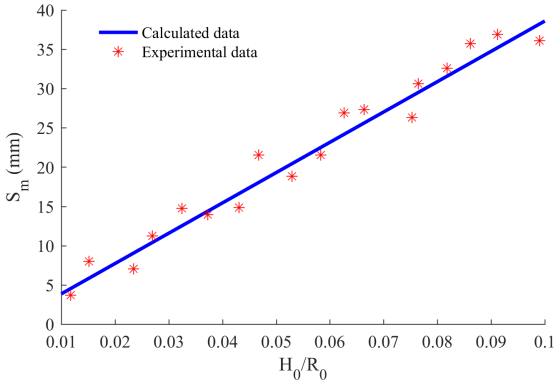

Figure 6: Maximum deflection varies with depth-to-width ratio

indicates the maximum deflection displacement increases linearly with the increase of depth-to-width ratio. According to the equation (10), the depth-to-width ratios of mitigated sites can be obtained based on the measured maximum deflection displacement. The mitigated sites left from the mitigation process by CO_2 laser which will result in light modulation to the downstream optics and the modulation intensity is affected by the morphology of mitigated sites. Thus, the morphology characteristics of mitigated sites obtained by beam deflection method could assess instantaneously damage resistance of the downstream optics in situ.

4 Conclusion

In this work, a method of beam deflection is developed by adjusting the incident way of the probe beam. The damage threshold of fused silica was quickly detected, with

the same result as the one obtained by applying the phase contrast microscope. Then the deflection displacements of the mitigated sites were measured and the morphologies of mitigated sites were analyzed. A method to quickly detect damage threshold of the fused silica components and the morphology characteristics of mitigated sites is proposed, which can provide significant reference as to the online assessment of the damage resistance of the downstream optics and provides the guidance of the repair process.

Acknowledgement: This work is supported in part by National Natural Science Foundation of China (No. 61505171), a project supported by Scientific Research Fund of Sichuan Provincial Education Department, China (No. 18CZ0014), and was also supported in part by National Nuclear Energy Development Project of China (No. 18zg6103).

References

[1] Spaeth M., Wegner P., Suratwala T., Optics recycle loop strategy for NIF operations above UV laser-induced damage threshold, Fusion. Sci. Technol., 2016, 69(1), 265-294.

[2] Manes K., Spaeth M., Adams J., Damage mechanisms avoided or managed for NIF large optics, Fusion. Sci. Technol., 2016, 69(1), 146-249.

[3] Gao X., Qiu R., Wang K., The size prediction of potential inclusions embedded in the subsurface of fused silica by damage morphology, Open. Phys., 2017, 15(1), 233-239.

[4] Gao X., Feng G., Han J., Investigation of laser-induced damage by various initiators on the subsurface of fused silica, Opt. Express., 2012, 20(20), 22095-22101.

[5] Lamaignère L., Bouillet S., Courchinoux R., An accurate, repeatable, and well characterized measurement of laser damage density of optical materials, Rev. Sci. Instrum., 2007, 78(10),290-291.

[6] Douti D. B., Chrayteh M., Aknoun S., Quantitative phase imaging applied to laser damage detection and analysis, Appl. Opt., 2015, 54(28), 8375-8382.

[7] Zhao D., Su J., Xu J., Plasma spectrum peak extraction algorithm of laser film damage, P-roc. SPIE., 2012, 8417, 349-356.

[8] Smith A. V., Do B. T., Bulk and surface laser damage of silica by picosecond and nanosecond pulses at 1064 nm, Appl. Opt., 2008, 47(26), 4812-4832.

[9] Gao X., Jiang Y., Qiu R., Effect of the repaired damage morphology of fused silica on the modulation of incident laser, Opt. Mater., 2017, 64, 295-301.

[10] Somoskoi T., Vass C., Mero M., Comparison of simultaneous online optical and acoustic laser damage detection methods in the nanosecond pulse duration domain, Laser. Phys., 2015, 25(5), 056002.

[11] Starke A. A., Bernhardt A., Laser damage threshold measurement according to ISO 11254 experimental realization at 1064 nm, Proc. SPIE., 1994, 2114, 212-219.

[12] Melninkaitis A., Balachninaite O., Rakickas T., Automated test station for laser-induced damage threshold measurements according to ISO 11254-2 standard, Proc. SPIE., 2006, 6101(2), 62-65.

[13] Petzoldt S., Elg A. P., Reichling M., Surface laser damage thresholds determined by photoacoustic deflection, Appl. Phys. Lett., 1988, 53(21), 2005-2007.

[14] Alvisi M., Giulio M. D., Marrone S. G., HfO_2 films with high laser damage threshold, Thin. Solid. Films., 2000, 358(1–2), 250-258.

[15] Perrone M. R., Piegari A. M., Masetti E., Laser damage threshold of MgF_2 thin films byphotoacoustic beam deflection, Proc. SPIE., 2000, 3902, 175-181.

[16] Riede W., Allenspacher P., TIR based photothermal/photoacoustic deflection, Proc. SPIE., 2008, 7132, 71320S.

[17] Cormont P., Combis P., Gallais L., Removal of scratches on fused silica optics by using a CO_2 laser, Opt. Express., 2013, 21(23), 28272-28289.

[18] Doualle T., Gallais L., Cormont P., Thermo-mechanical simulations of CO_2 laser–fuse dsil-ica interactions, J. Appl. Phys., 2016, 119(11), 2824-2145.

[19] Chunming L., Yong J., Chengsi L., The Structure Evolution of Fused Silica Induced by CO_2 Laser Irradiation. Chinese. Phys. Lett., 2012, 29(4), 44211-44214.

[20] Fang Z., Zhao Y. A., Sun W., CO_2 laser mitigation of the ultraviolet laser damage site on a fused silica surface, Opt. Eng., 2014, 53(8), 084107.